Advanced Journal of Chemistry, Section A

Journal homepage: www.ajchem-a.com

Original Research Article

Evaluation of Apremilast as a Potential Inhibitor of Activated Factor XII: *In Vitro* and *In Silico* Approaches

Hassan A. Madkhali[1]*, Mohd Nazam Ansari[1], Yassine Riadi[2], Majid A. Ganaie[3], Abdullah Y. Hamadi[4], Naif M. Alhawiti[5,6]

[1]*Department of Pharmacology & Toxicology, College of Pharmacy, Prince Sattam Bin Abdulaziz University, Al-Kharj, Saudi Arabia*
[2]*Department of Pharmaceutical Chemistry, College of Pharmacy, Prince Sattam Bin Abdulaziz University, 11942 Al-Kharj, Saudi Arabia*
[3]*College of Dentistry and Pharmacy, Buraydah Colleges, Buraydah, Saudi Arabia*
[4]*Faculty of Applied Medical Sciences, Medical Laboratory Technology, University of Tabuk, Tabuk, Saudi Arabia*
[5]*Department of Clinical Laboratory Sciences, College of Applied Medical Sciences, King Saud bin Abdulaziz University for Health Sciences, Riyadh, Saudi Arabia*
[6] *King Abdullah International Medical Research Center, Ministry of National Guard for Health Affairs, Riyadh, Saudi Arabia*

ARTICLEINFO

Article history

Submitted: 2025-12-01
Revised: 2026-01-05
Accepted: 2026-01-25
ID: AJCA-2512-2009
DOI: 10.48309/AJCA.2026.566309.2009

KEYWORDS

Factor XIIa
Apremilast
In vitro
In silico
Dynamic molecular
SASA

ABSTRACT

This study aimed to evaluate the inhibitory effects of apremilast on activated coagulation factor XII (FXIIa) using chromogenic enzyme assays and to examine molecular interactions between apremilast and benzamidine with the target protein 6I63 (FXIIa) through *in silico* techniques including docking, structural analyses, and dynamic simulations. The interaction strength of these complexes, focusing on hydrogen bonds, root mean square deviation (RMSD), root mean square fluctuation (RMSF), and solvent accessible surface area (SASA), was analyzed. Additionally, the selectivity of apremilast toward FXIIa over other related serine proteases (FIXa, FXa, FXIa, and plasma kallikrein) was determined using chromogenic assays. The findings indicated that apremilast has a significant inhibitory effect on FXIIa, while no notable effects were observed on the other proteases, suggesting selectivity for FXIIa. Furthermore, apremilast showed stronger binding affinity with 6I63 (−6.9 kcal/mol) compared to benzamidine (−5.3 kcal/mol), indicating a more stable and specific interaction. Apremilast induced greater compactness and stability of the complex, with lower RMSD and SASA values, whereas benzamidine favored a more flexible and less stable interaction. These results highlight distinct mechanisms by which each ligand interacts with FXIIa and provide insights into their therapeutic potential, suggesting apremilast could be effective in treating FXIIa-related diseases. In addition, ADME analysis revealed that benzamidine has better solubility, intestinal absorption, and excretion, while apremilast exhibits superior oral absorption and stronger inhibition of cytochrome P450 enzymes. Toxicity studies showed both compounds are mutagenic. Taken together, apremilast could serve as a lead compound for developing new therapeutic agents targeting FXIIa-related diseases.

* Corresponding author: Madkhali, Hassan A.
✉ E-mail: h.madkhali@psau.edu.sa
© 2026 by SPC (Sami Publishing Company)

GRAPHICAL ABSTRACT

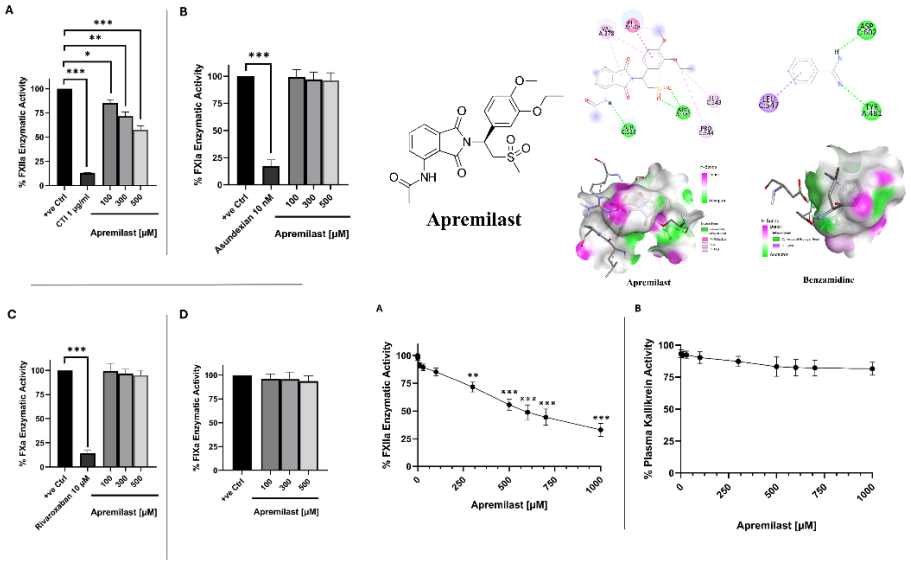

Introduction

Factor XIIa (FXIIa), a serine protease enzyme involved in the activation of the intrinsic coagulation pathway, is critical to hemostasis. This factor is essential for the activation of the coagulation cascade, which is a biological process that leads to the appearance of a blood clot to stop bleeding after the injury of a vascular vessel [1]. FXII is activated from its precursor, the FXII zymogen, upon surface pacing with negatively charged particles, usually also alongside high molecular weight kininogen (HMWK) and plasma prekallikrein (PPK) [2]. This causes minimal amounts of FXIIa to be generated, before there is further activation of FXIIa leading to plasma kallikrein (PK) activation. The active PK simultaneously also amplifies the response by activating more FXIIa [3].

After its generation, FXIIa propagates a series of enzymatic cascades notably activating factor XI (FXI) to FXIa and subsequently factor IX (FIX) to FIXa [1]. This enzymatic cascade is necessary for generating thrombin, which promotes the transformation of fibrinogen into fibrin, the main constituent of the blood clot [2]. In fact, FXII deficiency is not associated with impaired hemostasis, implying that FXIIa, while important for the process of coagulation, is not essential for maintaining physiologic hemostasis [3]. FXIIa can elicit a pro-inflammatory response via the kallikrein-kinin pathway through cleaving HMWK to liberate bradykinin, via this pathway that causes vasodilation and increases vascular permeability to drain to inflammation [4]. Inhibition of FXIIa is a mechanism to intercept the coagulation cascade early and to limit the generation of damaging thrombi with a lower risk of bleeding [5].

Apremilast is an orally active small molecule inhibitor of phosphodiesterase-4 (PDE4) that has demonstrated efficacy in the treatment of psoriatic arthritis (PsA) [6]. Apremilast has received approval for the treatment of active PsA in adults in multiple countries [7,8]. Recently, apremilast showed cardiometabolic beneficial effects in patients suffering from psoriasis associated with cardiometabolic diseases [9,10].

Apremilast has demonstrated significant anti-inflammatory effects by increasing intracellular cyclic adenosine monophosphate (cAMP) levels and inhibiting the production of pro-inflammatory cytokines [11,12]. The goal of this study is to deliver valuable data that lead to the

future design of novel therapeutic molecules, which specifically modulate FXIIa activity with little interference in hemostatic physiology [13].

Materials and Methods

Drugs and chemicals

Human enzymes, α-FXIIa, FXIa, plasma kallkrein, and the FXIIa inhibitor, corn trypsin inhibitor (CTI), were purchased from Enzyme Research Laboratories (South Bend, IN, USA). S2302, S2366, and CS-51(09) substrates were procured from Aniara (Mason, OH, USA). Apremilast and the plasma kallkrein inhibitor, aprotinin were obtained from Sigma-Aldrich (St. Louis, MO, USA). Asundexian was purchased from MCE (MedChemExpress, Monmouth Junction, NJ, USA).

Inhibition of coagulation FXIIa by Apremilast in enzyme assays

The aim of this study was to ascertain whether apremilast could exhibit any inhibitory effect on the activity of FXIIa protein. In combination with 0.5 mM S2302, 9 nM of activated FXII was utilized. The enzyme FXIIa and the substrate S2302 controls were utilized as baseline comparisons for the variable that was being investigated. The FXIIa control sample solely included FXIIa, a HEPES buffer with a pH of 7.1, and S2302. The components of the S2302 negative control were the HEPES buffer and the appropriate substrate. Apremilast concentrations used initially for screening were 100, 300, and 500 µM. Apremilast concentration range used in the dose response is 1, 1-1,000 µM. The rate of p-nitrophenylphosphate hydrolysis was measured at 405 nm using a BioTek ELx800 Absorbance microplate instrument (Marshall Scientific, Hampton, NH, USA) in conjunction with the BioTek Gen5 software (version 3.10, BioTek, Winooski, VT) [14,15]. Study observations are obtained in triplicate from minimum three independent experiments.

Selectivity of Apremilast for different serine proteases (FIXa, FXa, FXIa, and PK) in enzyme assays

An enzyme assays were equipped to assess the effects of apremilast, in the presence of other serine proteases; FIXa, FXa, FXIa, or PK. The enzymes and chromogenic substrates final concentrations are: 89 nM FIXa/ 0.85 mM CS-51(09), 150 nM FXa/ 0.4 mM S-2732, 2 nM FXIa/ 0.5 mM S-2366, and 2 nM PK/ 0.5 mM S-2302. The effect of different concentrations of apremilast (100, 300, and 500 µM) on targeted serine proteases was determined by mixing apremilast with a specific enzyme with its chromogenic substrate in HEPES-carbonated buffer. For PK assay, different concentrations of apremilast (1-1,000 µM) on PK were determined by mixing apremilast with the enzyme and its chromogenic substrate. CTI, asundexian, rivaroxaban, and aprotinin inhibitors were used as reference inhibitors for FXIIa, FXIa, FXa, and PK, respectively. Substrate hydrolysis and release of the product p-nitroaniline (pNA) resulted in an increase in absorbance. The concentrations of all coagulation proteins were finalized, and the change in absorbance was detected at 405 nm using the same above-mentioned absorbance microplate instrument [14,15]. At least three separate experiments were performed in a triplicate.

Molecular docking calculation procedure

The molecular docking calculation was performed using AutoDock Vina [16-18]. The protein and ligand files are converted to PDBQT format using AutoDockTools [19], adding the necessary charges and rotatable torsions. Next, a docking grid is configured and defined by the coordinates of the center of the docking box (center_x = 25.662, center_y = 41.254, and center_z = 21.611) and the grid size (size_x = 60, size_y = 60, and size_z = 60) according to the targeted interaction area on the protein [20,21].

The other parameters, such as the energy range (energy_range = 4) and exhaustiveness (exhaustiveness = 8), control the search depth and the number of poses generated, respectively. Once the grid and configuration are prepared, the docking configuration file (ligand.dpf) is created, specifying the protein file, the ligand, and the grid. The docking calculation is then launched with the appropriate command in the terminal. After the calculation is executed, the results, including the affinity scores and the generated poses, are recorded in a log file. These results visualized using tools like PyMOL and Discovery Studio [22-24].

Molecular dynamics simulation

Protein and protein-ligand complex microscopic stability is assessed using molecular dynamics, an advanced automated simulation method. Structure, function, fluctuation, interaction, and behavior are demonstrated to do this. The behavior of the two complexes was investigated using GROMACS version 2023.1 for MD calculations [25,26]. CHARMM General Force Field parameterized protein content. The SwissParam server implemented ligand topologies [27]. The structures were vacuum minimized 2,500 times using steepest descent to address steric issues. The SPC water model solvated the structure; after adding Na^+ and Cl^- ions, the gmx genion instrument balanced the system. This was done to ensure system electrical neutrality. After minimization, MD simulations went into production, NVT, and NPT. Two phases balanced the systems. First, a 100 picosecond NVT equilibration was done to maintain particle number, volume, and temperature. The procedure aimed to raise system temperature to 300 kelvins. The second stage involved a precise 100 picosecond NPT equilibration to achieve temperature, pressure, and particle number homogeneity. It was essential to maintain system density and pressure. The protein group's location was limited by bond limitations on all bonds during simulations. The system entropy reduced because NVT and NPT restricted water molecules around the protein, relaxing them. Parrinello-Rahman barostat method and v-rescale thermostat for molecular dynamics [28]; the thermostat and barostat were adjusted for 100 picoseconds. To constrain covalent bonding, the Linear Constraint Solver application was used. Chemical bond interactions were handled using the sophisticated (Particle-Mesh Ewald) or PME approach. Every system has a 100-ns production run after equilibrium.

Statistical analysis

Independent experiments were conducted at least three times and data then were collected. The mean ± SEMs from the bioassays of FXlla, PK, and FXIa were evaluated using GraphPad Prism 10.0 (GraphPad Software, Inc., San Diego, CA, USA) through nonlinear regression analysis. A one-way analysis of variance (ANOVA) followed by Dunnett's post hoc test was employed to analyze the data. Statistical significance for all comparisons was determined at $p < 0.05$.

Results and Discussion

Apremilast effects on FXIIa and other protease enzymes

Initially, screening experiments were conducted to assess the possible inhibitory effects of apremilast on the targeted protein; FXIIa at selected concentrations (100, 300, and 500 μM) using chromogenic assays.

Three independent chromogenic assays were conducted in triplicate. FXIIa inhibitor, corn trypsin inhibitor was used as reference inhibitor. These findings indicated that apremilast significantly inhibited the activity of FXIIa enzyme (Figure 1A).

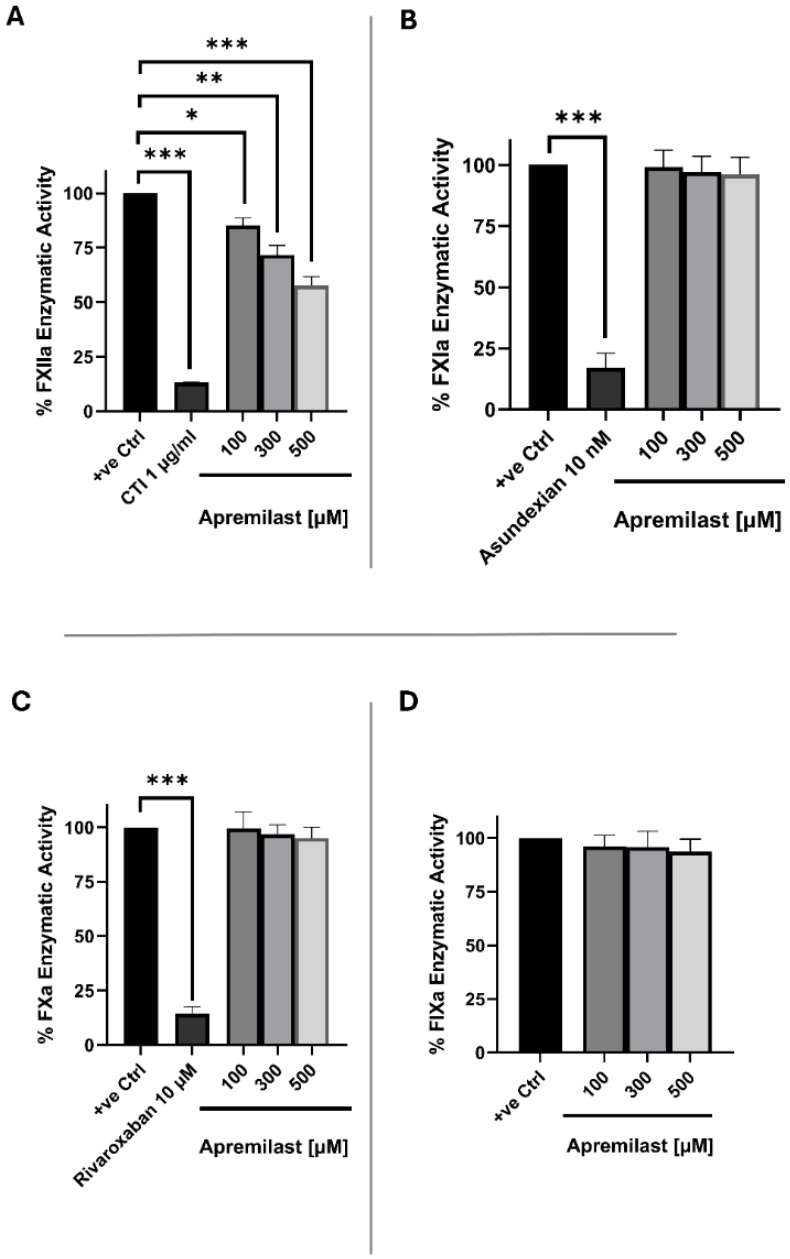

Figure 1. Effect of apremilast on FXIIa and other coagulation factors; FXIa, FXa, and FIXa. (A) Effects of apremilast on FXIIa activity. FXIIa enzyme and S2302 substrate (0.5 mM) were incubated in the absence or presence of 100, 300, and 500 µM concentrations of apremilast and 1 µg/mL of CTI, a reference inhibitor. (B) Effects of apremilast on FXIa activity. FXIa enzyme and S2366 substrate (0.5 mM) were incubated in the absence or presence of 100, 300, and 500 µM concentrations of apremilast and 10 nM of asundexian, a reference inhibitor. (C) Effects of apremilast on FXa activity. FXa enzyme and S2732 substrate (0.4 mM) were incubated in the absence or presence of 100, 300, and 500 µM concentrations of apremilast and 10 µM of rivaroxaban, a reference inhibitor. (D) Effects of apremilast on FIXa activity. 89 nM FIXa enzyme and CS-51(09) substrate (0.85 mM) were incubated in the absence or presence of 100, 300, and 500 µM concentrations of apremilast. For all panels, data are expressed as % mean ± SEM for three independent triplicate experiments. *$p \leq 0.05$, **$p \leq 0.01$, and ***$p \leq 0.001$ compared to FXIIa-S2302 samples without inhibitor

Furthermore, the selectivity of apremilast to FXIIa was also assessed over other related coagulation FXIa, FXa, and FIXa enzymes and indicated that no significant effects on these enzymes, suggesting a selective inhibitory effect of apremilast on the targeted protein FXIIa (Figure 1(B, C, and D)).

Dose-response effects of apremilast on FXIIa and PK enzymes

A dose-response curve for apremilast on FXIIa to explore the dose-dependent effects and determine the IC_{50} of the drug. The results exhibited that apremilast has dose-dependent inhibitory effects on FXIIa activity with IC_{50} equal to 479.6 µM (Figure 2A). To further benchmark this IC_{50} value, it is useful to compare it with the known human plasma exposures of apremilast. Apremilast reaches a C_{max} of approximately 0.8–0.9 µM at the approved therapeutic dose of 30 mg twice daily, more than 500-fold lower than its IC_{50} in the FXIIa inhibition assay. This large difference suggests that apremilast does not directly inhibit FXIIa at clinically achievable concentrations. Accordingly, for the future optimization of apremilast as lead compound the results should be viewed not as evidence supporting immediate clinical dose finding but rather as description of an attractive chemical scaffold. PK plays a significant role in the pathogenesis of inflammatory conditions, including PsA. The kallikrein-kinin system (KKS) is activated in various inflammatory diseases, contributing to the chronic inflammation observed in PsA [29]. PPK, the precursor of PK, is activated by factor XII, leading to the regulation of multiple proteolytic cascades in the cardiovascular system [30,31]. Furthermore, in KKS, FXII and PPK are reported to reciprocally activate one another to form their active forms: FXIIa and PK [30]. For all these reasons, a dose-response curve was also run for apremilast on PK and indicated that there are no significant effects on the activity of PK, an important activator of factor XII enzyme (Figure 2B).

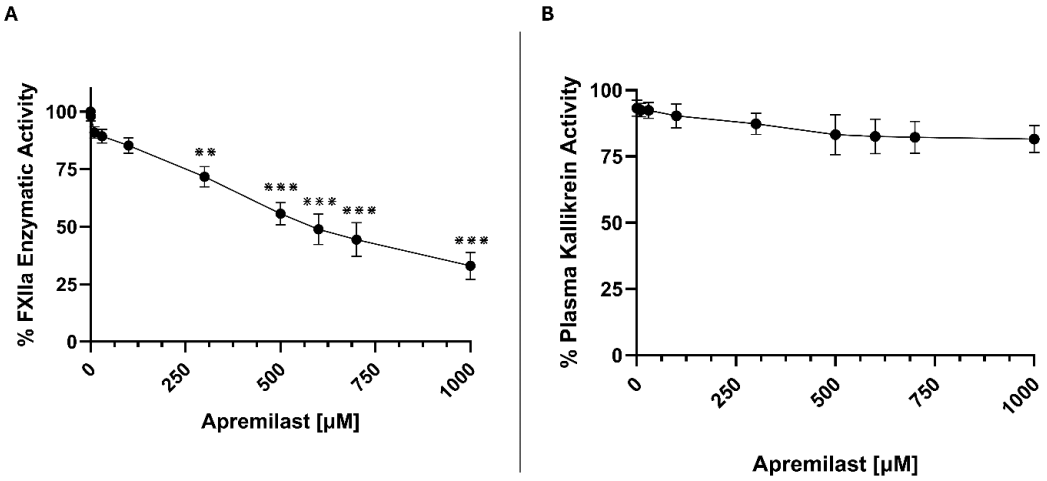

Figure 2. Representative dose-response curves for apremilast on FXIIa and PK enzymes (A) Effects of apremilast on FXIIa activity. 9 nM FXIIa enzyme and S2302 substrate (0.5 mM) were incubated in the absence or presence of 1, 10, 30, 100, 300, 500, 600, 700, and 1,000 µM concentrations of apremilast. (B) Effect of apremilast on PK activity. 2 nM PK enzyme and S2302 substrate (0.5 mM) were incubated in the absence or presence of 1, 10, 30, 100, 300, 500, 600, 700, and 1,000 µM concentrations of apremilast. For both panels, data are expressed as % mean ± SEM for three independent triplicate experiments. **p ≤ 0.01 and ***p ≤ 0.001 compared to FXIIa-S2302 samples without inhibitor

Docking scrutiny

In Figure 3, the 2D diagrams illustrate the specific interactions between the ligands and the protein residues, such as hydrogen bonds and hydrophobic interactions. Apremilast interacts with residues such as VAL (A378), PHE (A518), LEU (C543), and ARG (C381), while benzamidine primarily binds to ASP (C602) and TYR (A481). The 3D representations show the protein surface and the interaction zones, highlighting additional interactions such as π-π and π-alkyl interactions, which enhance the stability of the complexes. In Table 1, the affinity of apremilast is -6.9 kcal/mol, indicating a thermodynamically favorable interaction and a relatively strong binding between this ligand and the protein. On the other hand, the affinity of benzamidine -5.3 kcal/mol, is higher than that of apremilast, suggesting better specificity and stability of the ligand-protein complex compared to benzamidine.

Dynamic molecular

RMSD study

In Figure 4, the FXIIa–apremilast complex showed minimal fluctuations, with root mean square deviation (RMSD) values consistently maintained between 0.05 and 0.09 nm, suggesting strong structural stability throughout the 100 ns simulation.

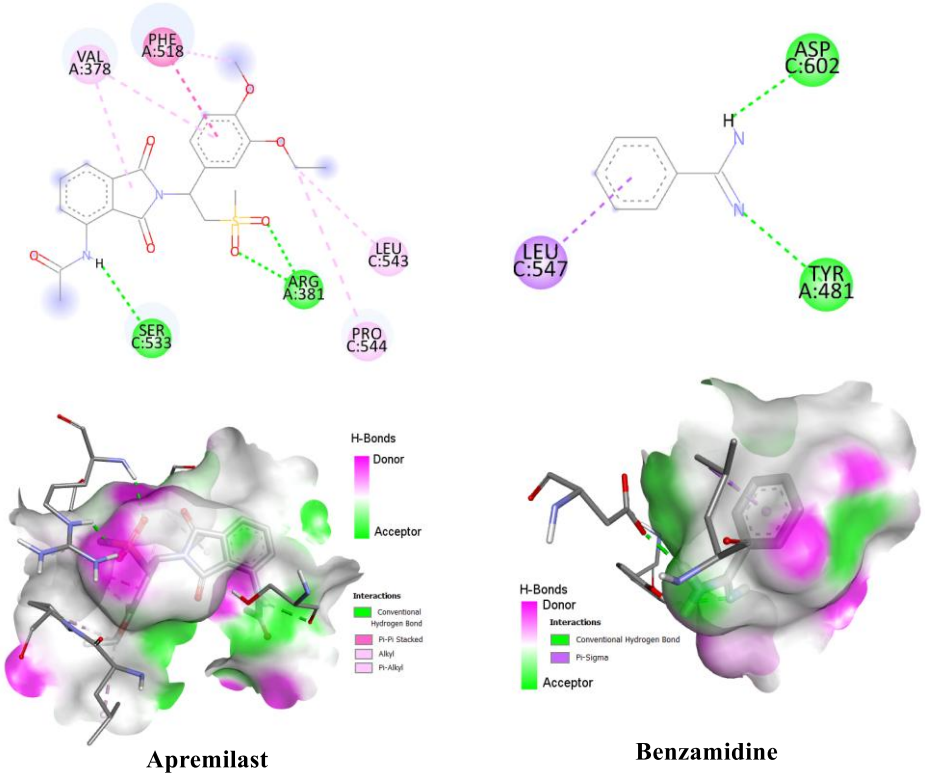

Figure 3. 2D and 3D molecular interactions between apremilast, benzamidine, and protein 6I63

Table 1. Affinity in kcal/mol of the interaction of apremilast and benzamidine with 6I63

	Affinity (kcal/mol)
Apremilast	-6.9
Benzamidine	-5.3

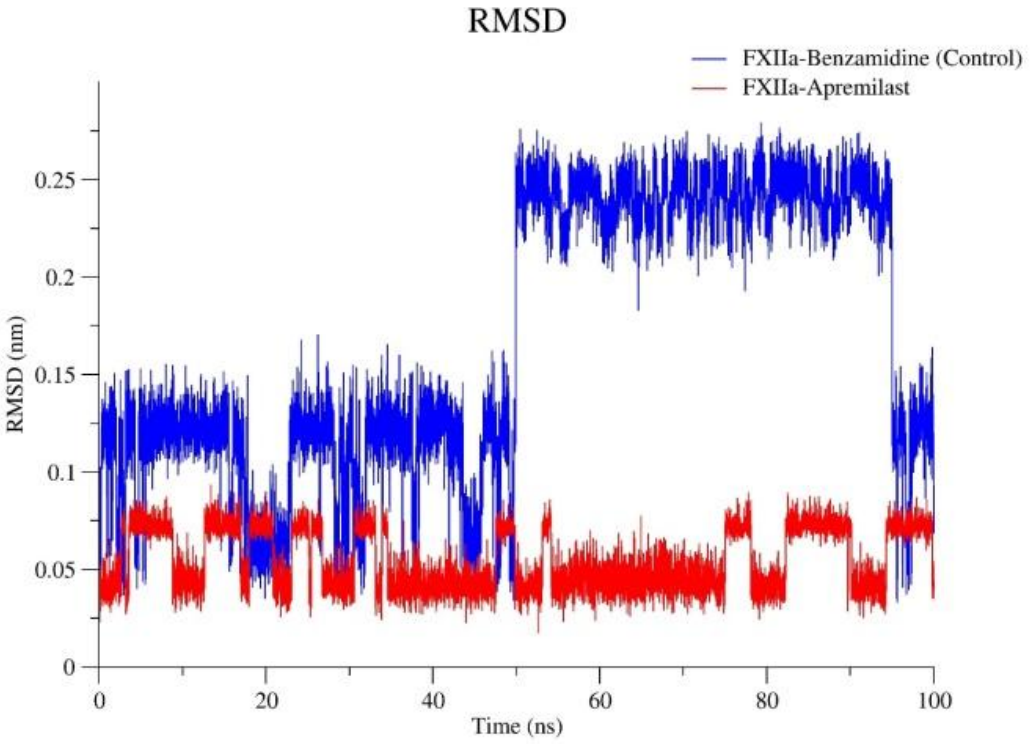

Figure 4. Comparison of the conformational stability of FXIIa-benzamidine and FXIIa-apremilast complexes

Conversely, the FXIIa–benzamidine complex displayed greater fluctuations with two distinct states: one between 0.1 and 0.15 nm in the early phase and another increased range between 0.22 and 0.28 nm during the later phase. This suggests that apremilast binding imposes more rigid stabilization on FXIIa compared to benzamidine. Thus, a plateau of RMSD values shows that the structure varies around a stable average conformation, as seen in all MD simulations. The MD trajectory parameters were analyzed using XmGrace [32,33]. Moreover, FXIIa-apremilast induces more moderate fluctuations compared to FXIIa-benzamidine, whose fluctuations are more marked and irregular. In summary, these results indicate that the interaction of FXIIa with apremilast is more robust and stabilizing compared to FXIIa-benzamidine, suggesting more therapeutic efficacy of apremilast.

Analysis of the conformational flexibility of FXIIa-benzamidine and FXIIa-apremilast complexes: RMSF evaluation

The local conformational flexibility of the FXIIa-benzamidine and FXIIa-apremilast complexes was analyzed using the root mean square fluctuation (RMSF) metric. Figure 5 displays the changes in the RMSF of the FXIIa-benzamidine and FXIIa-apremilast complexes. For the FXIIa-apremilast complex, the fluctuations are relatively low and homogeneous, with values averaging around 0.10 to 0.12 nm, suggesting greater structural rigidity and a reduction in conformational movements. In contrast, the FXIIa-benzamidine complex exhibits much greater fluctuations.

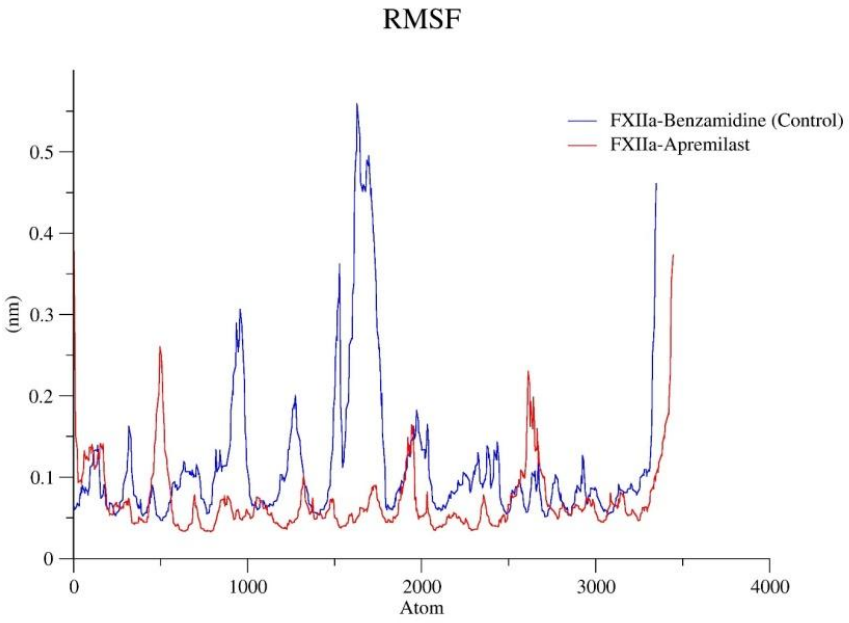

Figure 5. Root means square fluctuation

Certain regions of the protein show peak up to 0.54 nm, indicating greater conformational flexibility, which reflects a less rigid interaction allowing more room for structural adjustments within the protein. In summary, apremilast could confer increased stability to FXIIa, while benzamidine could lead to greater structural dynamics, potentially affecting the ligand's affinity and specificity. While benzamidine makes more and stronger hydrogen bonds within the FXIIa active site, this relationship does not necessarily hold for overall binding affinity, especially with low molecular weight ligands. The MD analysis demonstrates an overall compact and stable binding conformation of apremilast yet considering its larger size and hydrophobic character such stability measures have to be handled with care. For this reason, it was not claimed that apremilast binds more strongly than benzamidine and rather stress that the two ligands show different binding modes. A detailed free-energy decomposition analysis (*e.g.,* MM-PBSA with per-residue contributions) will be necessary in future studies to describe the relative contribution of hydrogen bonding versus hydrophobic packing within this loop.

Evaluation of the radius of gyration (Rg)

Figure 6, the data analysis shows that the FXIIa-apremilast complex has lower Rg values, ranging from 1.64 nm to 1.69 nm, with an average value of 1.665 nm, suggesting that this interaction helps maintain the protein in a more stable structure and less prone to large conformational movements.

In contrast, the FXIIa-benzamidine complex shows higher Rg values, ranging from 1.69 nm to 1.74 nm, with an average of approximately 1.715 nm, indicates a relatively less compact and more flexible structure compared to that of FXIIa-apremilast. In conclusion, the results suggest that FXIIa-apremilast induces a more compact and stable conformation of the protein, which could be a sign of a stronger and more specific interaction between the ligand and target compared to FXIIa-benzamidine complex.

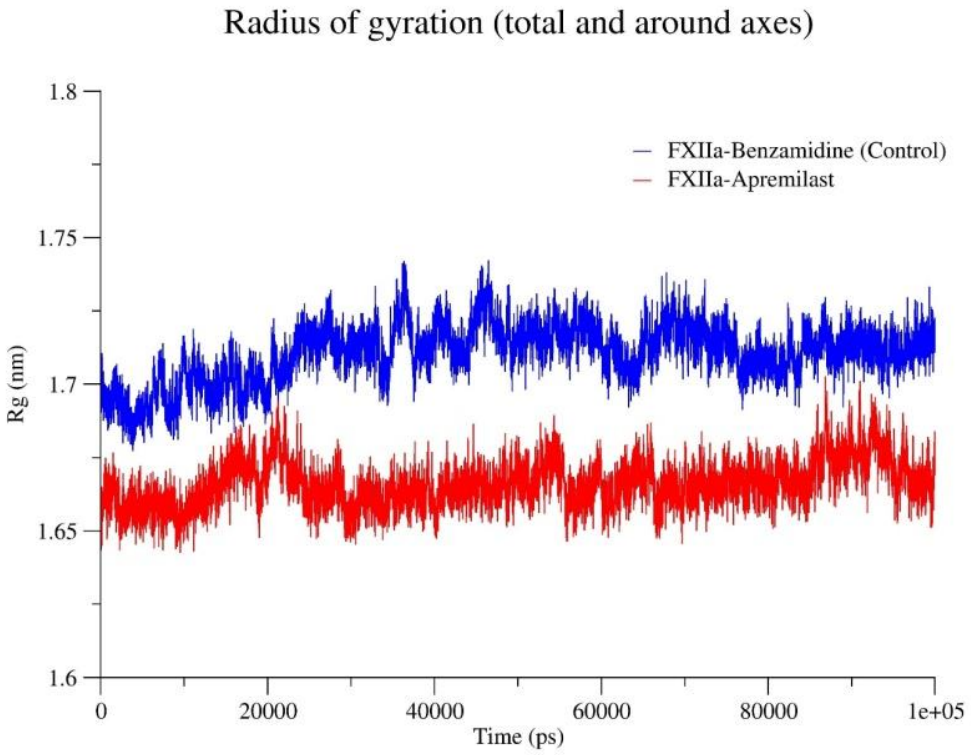

Figure 6. Rg of FXIIa-benzamidine and FXIIa-apremilast complexes

Analysis of the solvent accessible surface area (SASA) of the complexes

In Figure 7, the results show that the FXIIa-apremilast complex has lower SASA values, ranging between 105 and 112 nm^2, with an average around 110 nm^2, while the FXIIa-benzamidine complex shows higher SASA values, ranging from 112 to 123 nm^2, with an average around 118 nm^2.

The reduction of the solvent-accessible surface observed for FXIIa-apremilast suggests that this ligand could offer better stability and optimized pharmacokinetic properties compared to FXIIa-benzamidine, thereby enhancing its potential as a therapeutic treatment.

Analysis of hydrogen bond formation in the complexes

In Figure 8, the results indicate that benzamidine forms more consistent and structured hydrogen bonds, suggesting a more stable and stronger interactions with FXIIa. Apremilast, with less frequent hydrogen bond formation, might bind to the FXIIa protein in a more dynamic and flexible manner, likely favoring hydrophobic interactions. These differences in the types of interactions can influence the stability and specificity of the complexes, which could have consequences on their therapeutic efficacy and mode of action in biological environments.

ADMET study

By analyzing ADMET (absorption, distribution, metabolism, excretion, and toxicity), data help predict the efficacy, safety, and tolerance of a drug.

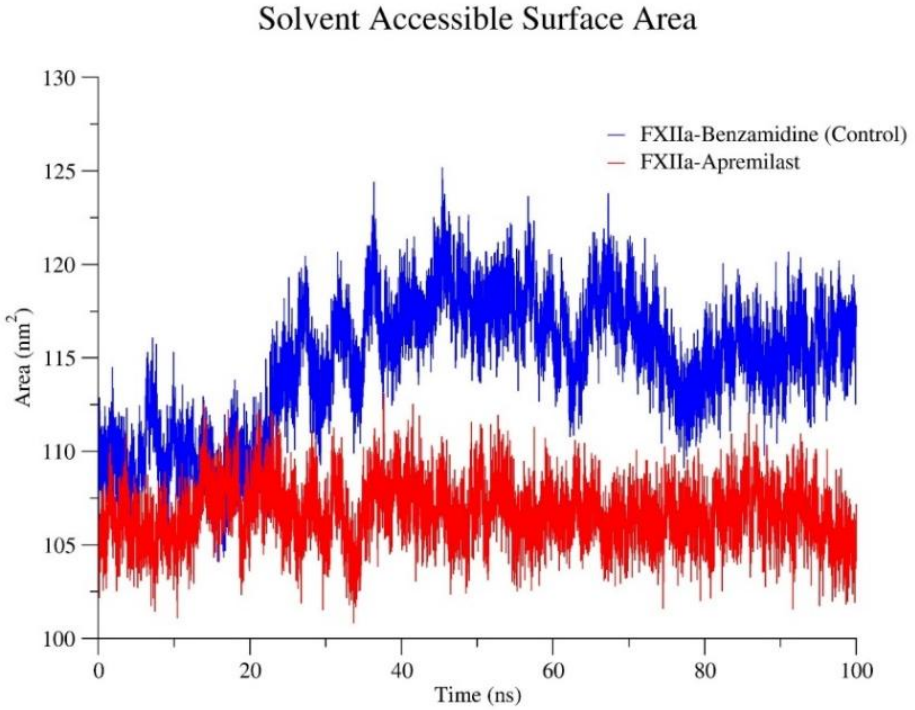

Figure 7. SASA of FXIIa-benzamidine and FXIIa-apremilast complexes during the simulation

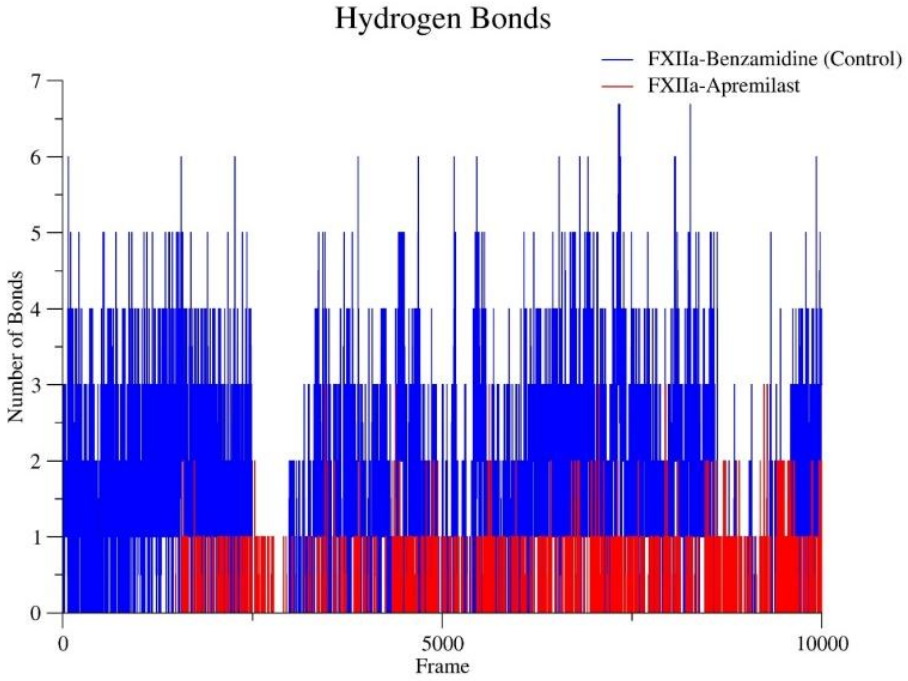

Figure 8. Formation of hydrogen bonds in the FXIIa-Benzamidine and FXIIa-Apremilast complexes during the simulation

Table 2. The ADME parameters of apremilast and benzamidine

ID	Apremilast	Benzamidine
BBB	0.0963193	1,55774
Buffer_solubility_mg_L	48.1117	4953,89
$CaCO_2$	5,37653	19,4323
CYP_2C19_inhibition	Non	Inhibitor
CYP_2C9_inhibition	Inhibitor	Inhibitor
CYP_2D6_inhibition	Non	Inhibitor
CYP_2D6_substrate	Non	Substrate
CYP_3A4_inhibition	Inhibitor	Non
CYP_3A4_substrate	Substrate	Weakly
HIA	98,046458	81,769379
MDCK	0.623688	34,2282
Pgp_inhibition	Inhibitor	Non
Plasma_Protein_Binding	83,840393	0.000000
Pure_water_solubility_mg_L	0.742883	10283,4
Skin_Permeability	-2.34367	-2,99553
SKlogD_value	1,6378	-1,02685
SKlogP_value	1,6378	0.801280
SKlogS_buffer	-3.980980	-1,38479
SKlogS_pure	-5,79231	-1,0676

In Table 2, in terms of solubility in a buffer, benzamidine shows a much higher value (4953.89 mg/L) than apremilast (48.1117 mg/L), which suggests better solubility for the former. Regarding intestinal absorption (measured by Caco-2), benzamidine also shows a higher absorption capacity (19.4323) compared to apremilast (5.37653). Apremilast exhibits superior oral absorption (HIA) (98.046458%) compared to benzamidine (81.769379%), indicating better absorption when administered orally. Regarding the disposition in the body, apremilast inhibits several cytochrome P450 enzymes (notably CYP 2C9 and CYP 3A4), while benzamidine primarily inhibits CYP 2C9 and CYP 2D6. Apremilast is also a substrate for CYP 3A4, whereas benzamidine is a weak substrate. In terms of plasma protein binding, apremilast binds strongly (83.840393%), whereas benzamidine shows no detectable binding, which could influence their distribution and efficacy. Regarding skin permeability, both compounds have similar values, indicating a low ability to penetrate the skin. Regarding excretion, benzamidine shows higher renal permeability, suggesting it could be excreted more efficiently. Finally, apremilast and benzamidine show similar values for their lipophilicity (LogP), but apremilast has better membrane distribution (LogD) and lower solubility in pure water (LogS), which may affect their respective pharmacokinetics. In summary, benzamidine might have better solubility and more efficient excretion, while apremilast shows better oral absorption and a more pronounced inhibition of cytochrome P450 enzymes [34].

In Table 3, regarding the toxicity to algae, benzamidine shows a higher value (0.181011) than apremilast (0.0659196), suggesting greater toxicity. Both compounds are mutagenic according to the Ames test, indicating their potential to induce genetic mutations.

Table 3. Toxicity and mutagenicity tests of apremilast and benzamidine

ID	Apremilast	Benzamidine
algae_at	0.0659196	0.181011
Ames_test	Mutagen	Mutagen
Carcino_Mouse	Negative	Negative
Carcino_Rat	Negative	Negative
daphnia_at	0.133751	1.0682
hERG_inhibition	Low_risk	Medium_risk
medaka_at	0.0430278	1.25975
minnow_at	0.0548672	0.518703
TA100_10RLI	Positive	Negative
TA100_NA	Negative	Negative
TA1535_10RLI	Negative	Negative
TA1535_NA	Negative	Negative

In terms of carcinogenicity, neither apremilast nor benzamidine showed any carcinogenic effects in mouse and rat models. Regarding Daphnia toxicity, Benzamidine shows a significantly higher value (1.0682) than apremilast (0.133751), which suggests greater aquatic toxicity for Benzamidine. Regarding hERG inhibition, apremilast presents a low risk, while benzamidine presents a medium risk, suggesting a more potential for cardiac disorders. For the medaka fish, benzamidine is also more toxic (1.25975) compared to apremilast (0.0430278). Similarly, benzamidine is more toxic to the minnow fish (0.518703) than apremilast (0.0548672). Finally, in the TA100 10RL tests, apremilast shows a positive effect (mutagenic), while benzamidine is negative. However, in other bacterial mutation tests (TA100 NA, TA1535 10RL, and TA1535 NA), both showed no mutagenic effects. In summary, although both compounds exhibit mutagenic potential, benzamidine appears to be more toxic, while apremilast shows a more pronounced risk in the bacterial mutation test. It is important to note that the *in silico* Ames prediction (TA100_10RLI) does not align with the extensive preclinical and clinical safety data available for apremilast. Regulatory toxicology studies have consistently shown that apremilast is negative in standard genotoxicity assays, including Ames tests, chromosome aberration assays, and *in vivo* micronucleus tests, and no genotoxicity or carcinogenicity signals have been identified in humans. This discrepancy highlighted the known limitations of computational toxicity models and reinforces that *in silico* predictions must be interpreted alongside established experimental safety evidence.

Conclusion

In the current study, the significant dose-dependent inhibitory effects of the oral PDE4 inhibitor apremilast were shown on the FXIIa activity using *in vitro* chromogenic assays. Additionally, the analysis of molecular interactions between apremilast and benzamidine with the 6I63 protein reveals that apremilast forms a more stable and specific complex compared to benzamidine. The stronger binding affinity, associated with lower values of RMSD, SASA, and Rg, suggests that apremilast induces a more compact and rigid structure. This could enhance its therapeutic potential by strengthening the stability and specificity of its interaction with the target protein. On the other hand, benzamidine exhibits greater flexibility, which led to less stable interactions and reduced binding affinity. These results highlighted the

importance of molecular dynamics in understanding the stability and flexibility of the interactions between apremilast and its target, showing that apremilast could be an effective drug for treating diseases related to FXIIa. Overall, although apremilast is not a potent inhibitor of FXIIa, this finding could uncover other anti-inflammatory mechanisms of apremilast in PsA and FXIIa-related inflammatory conditions. Considering the large difference between the IC_{50} value obtained *in vitro* and the clinically achieved plasma concentrations of apremilast, the compound should not be considered a directly repurposable FXIIa inhibitor at therapeutic doses. Instead, the data support the role of apremilast as a preliminary 'hit' or structural starting point for designing more potent FXIIa inhibitors. Taken together, this repositioning perspective aligns with the modest docking score advantage and the qualitative stability observed in MD simulations, which collectively suggest that the apremilast scaffold warrants further optimization rather than immediate translational application. In addition, apremilast could also serve as a lead compound for developing more potent therapeutic agents to be used for the prevention of FXIIa-associated inflammatory diseases.

Acknowledgments

The authors are thankful to the Department of Pharmacology and Toxicology, College of Pharmacy, PSAU, for providing the facility to perform the study.

Authors' Contributions

HAM designed the research study. HAM, MNA, and YR performed the research. HAM, MAG, and MNA analyzed the data. HAM, YR, AYH, and NMA wrote the manuscript. All authors participated sufficiently in the work and agreed to be accountable for all aspects of the work. All authors read and approved the final manuscript.

Funding

The authors would like to extend their appreciation to Prince Sattam bin Abdulaziz University for funding this research work through the project number (PSAU/2025/03/34701).

Data availability

Data supporting the findings of this study are available upon reasonable request from the corresponding author.

Conflict of Interest

The authors declared no conflict of interest.

ORCID

Hassan A. Madkhali:
https://orcid.org/0000-0002-0267-4194
Mohd Nazam Ansari:
https://orcid.org/0000-0001-8580-3002
Yassine Riadi:
https://orcid.org/0000-0002-5128-0765
Majid A. Ganaie:
https://orcid.org/0000-0001-6895-5370
Abdullah Y. Hamadi:
https://orcid.org/0000-0002-1095-5455
Naif M. Alhawiti:
https://orcid.org/0000-0002-8357-6886

References

[1] Danese, E., Montagnana, M., Lippi, G. Factor XII in hemostasis and thrombosis: active player or (innocent) bystander?. *Seminars in Thrombosis and Hemostasis*, **2016**, 42(6), 682–688.
[2] Reddigari, S.R., Shibayama, Y., Brunnée, T., Kaplan, A.P. Human Hageman factor (factor XII) and high molecular weight kininogen compete for the same binding site on human umbilical vein endothelial cells. *The Journal of Biological Chemistry*, **1993**, 268(16), 11982–11987.
[3] Gailani, D., Renné, T. Intrinsic pathway of coagulation and arterial thrombosis. *Arteriosclerosis, Thrombosis, and Vascular Biology*, **2007**, 27(12), 2507–2513.

[4] Schmaier, A.H., McCrae, K.R. The plasma kallikrein-kinin system: Its evolution from contact activation. *J Thromb Haemost,* **2007**, 5(12), 2323-2329.
[5] Dorgalaleh, A., Hosseini, M. S., Mobaraki, R. N., Alizadeh, S., Hosseini, S., Tabibian, S., Shamsizadeh, M., Moghaddam, E. S., Khosravi, S., Rahimizadeh, A. Inhibition of factor XIIa, a new approach in management of thrombosis. *Annals of Translational Medicine*, **2015**, 3(Suppl 1), S20.
[6] Reed, M., Crosbie, D. Apremilast in the treatment of psoriatic arthritis: A perspective review. *Therapeutic Advances in Musculoskeletal Disease*, **2017**, 9(2), 45–53.
[7] Poole, R.M., Ballantyne, A.D. Apremilast: First global approval. *Drugs*, **2014**, 74(7), 825–837.
[8] Blair, H.A. Apremilast: First pediatric approval. *Paediatric Drugs,* **2024**, 27(1), 119–124.
[9] Gelfand, J.M., Shin, D.B., Armstrong, A.W., Tyring, S.K., Blauvelt, A., Gottlieb, S., Lockshin, B.N., Kalb, R.E., Fitzsimmons, R., Rodante, J., Parel, P., Manyak, G.A., Mendelsohn, L., Noe, M.H., Papadopoulos, M., Syed, M.N., Werner, T.J., Wan, J., Playford, M.P., Alavi, A., Mehta, N.N. Association of apremilast with vascular inflammation and cardiometabolic function in patients with psoriasis: The VIP-a phase 4, open-label, nonrandomized clinical trial. *JAMA Dermatology*, **2022**, 158(12), 1394–1403.
[10] Cavanaugh, C., Orroth, K., Qian, X., Kumparatana, P., Klyachkin, Y., Colgan, S., Cordey, M. Diabetes and obesity burden and improvements in cardiometabolic parameters in patients with psoriasis or psoriatic arthritis receiving apremilast in a real-world setting. *JAAD International*, **2024**, 16, 244-251.
[11] Nassim, D., Alajmi, A., Jfri, A., Pehr, K. Apremilast in dermatology: A review of literature. *Dermatologic Therapy*, **2020**, 33(6), e14261.
[12] Monteiro, F., Vittal Shetty, V., Acharaya, R., Naresh, S., Munikumar, M., S Shetty, S., Nataranjan, P., Kumari N, S. Naringin from citrus maxima peel: A potential therapeutic agent for breast cancer via pkm2 inhibition. *Beni-Suef University Journal of Basic and Applied Sciences*, **2025**, 14(1), 78.
[13] Manne, M. Multitargeted therapy in the convergence era: Systems pharmacology, smart delivery, and the rise of pan-biomarkers. *Journal of Applied Pharmaceutical Science*, **2025**, 15(11), 001-007.
[14] Madkhali, H., Tarawneh, A., Ali, Z., Le, H.V., Cutler, S.J., Khan, I.A., Shariat-Madar, Z. Identification of human kinin-forming enzyme inhibitors from medicinal herbs. *Molecules*, **2021**, 26(14), 4126.
[15] Madkhali, H.A., Ansari, M.N., Alamri, M.A. Inhibition of activated coagulation factor xii by the phosphodiesterase-4 inhibitor roflumilast: In vitro and in silico studies. *Frontiers in Bioscience-Landmark*, **2025**, 30(5), 38395.
[16] Trott, O., Olson, A.J. Autodock vina: Improving the speed and accuracy of docking with a new scoring function, efficient optimization, and multithreading. *Journal of Computational Chemistry*, **2010**, 31(2), 455-461.
[17] Eberhardt, J., Santos-Martins, D., Tillack, A.F., Forli, S. Autodock vina 1.2. 0: New docking methods, expanded force field, and python bindings. *Journal of Chemical Information and Modeling*, **2021**, 61(8), 3891-3898.
[18] Ungarala, R., Munikumar, M., Sinha, S.N., Kumar, D., Sunder, R.S., Challa, S. Assessment of antioxidant, immunomodulatory activity of oxidised epigallocatechin-3-gallate (green tea polyphenol) and its action on the main protease of sars-cov-2—an in vitro and in silico approach. *Antioxidants*, **2022**, 11(2), 294.
[19] Morris, G.M., Huey, R., Lindstrom, W., Sanner, M.F., Belew, R.K., Goodsell, D.S., Olson, A.J. Autodock4 and autodocktools4: Automated docking with selective receptor flexibility. *Journal of Computational Chemistry*, **2009**, 30(16), 2785-2791.
[20] Ram, T.S., Munikumar, M., Raju, V.N., Devaraj, P., Boiroju, N.K., Hemalatha, R., Prasad, P., Gundeti, M., Sisodia, B.S., Pawar, S. In silico evaluation of the compounds of the ayurvedic drug, ayush-64, for the action against the sars-cov-2 main protease. *Journal of Ayurveda and Integrative Medicine*, **2022**, 13(1), 100413.
[21] Naik, V.R., Munikumar, M., Ramakrishna, U., Srujana, M., Goudar, G., Naresh, P., Kumar, B.N., Hemalatha, R., Remdesivir (gs-5734) as a therapeutic option of 2019-ncov main protease–in silico approach. *Journal of Biomolecular Structure and Dynamics*, **2021**, 39(13), 4701-4714.
[22] Lu, S.H., Wu, J.W., Liu, H.L., Zhao, J.H., Liu, K.T., Chuang, C.K., Lin, H.Y., Tsai, W.B., Ho, Y. The discovery of potential acetylcholinesterase inhibitors: A combination of pharmacophore modeling, virtual screening, and molecular docking studies. *Journal of Biomedical Science*, **2011**, 18(1), 8.
[23] Schrödinger, L., DeLano, W., PyMOL. **2020**.
[24] Manne, M., Goudar, G., Varikasuvu, S.R., Khetagoudar, M.C., Kanipakam, H., Natarajan, P., Ummiti, M.D., Yenagi, V.A., Chinthakindi, S., Dharani, P., Thota, D.S.S., Patil, S., Patil, V. Cordifolioside: potent inhibitor against Mpro of SARS-CoV-2 and immunomodulatory through human TGF-β and TNF-α. 3 Biotech, **2021**, 11, 136.
[25] Abraham, M.J., Murtola, T., Schulz, R., Páll, S., Smith, J.C., Hess, B., Lindahl, E. Gromacs: High performance molecular simulations through multi-level

parallelism from laptops to supercomputers. *SoftwareX*, **2015**, 1, 19-25.
[26] Pamu, D., Ayyamperumal, S., Manne, M., Tallapaneni, V., Moola, C.J.N., Karri, V.V.S.R. Preliminary hypothetical assessment and in silico molecular docking of statin to vegfr2 and vegfr3 protein complex associated with angiogenesis and lymphangiogenesis in diabetic wounds. *Journal of Applied Pharmaceutical Science*, **2023**, 13(1), 009-020.
[27] Zoete, V., Cuendet, M.A., Grosdidier, A., Michielin, O. Swissparam: A fast force field generation tool for small organic molecules. *Journal of Computational Chemistry*, **2011**, 32(11), 2359-2368.
[28] Ke, Q., Gong, X., Liao, S., Duan, C., Li, L. Effects of thermostats/barostats on physical properties of liquids by molecular dynamics simulations. *Journal of Molecular Liquids*, **2022**, 365, 120116.
[29] DeLa Cadena, R., Laskin, K.J., Pixley, R.A., Sartor, R.B., Schwab, J.H., Back, N., Bedi, G.S., Fisher, R.S., Colman, R.W. Role of kallikrein-kinin system in pathogenesis of bacterial cell wall-induced inflammation. *American Journal of Physiology-Gastrointestinal and Liver Physiology*, **1991**, 260(2), G213-G219.
[30] Kolte, D., Shariat-Madar, Z. Plasma kallikrein inhibitors in cardiovascular disease: An innovative therapeutic approach. *Cardiology in Review*, **2016**, 24(3), 99-109.
[31] Varikasuvu, S.R., Thangappazham, B., Vykunta, A., Duggina, P., Manne, M., Raj, H., Aloori, S. Covid-19 and vitamin d (co-vivid study): A systematic review and meta-analysis of randomized controlled trials. *Expert Review of Anti-Infective Therapy*, **2022**, 20(6), 907-913.
[32] Knapp, B., Frantal, S., Cibena, M., Schreiner, W., Bauer, P. Is an intuitive convergence definition of molecular dynamics simulations solely based on the root mean square deviation possible? *Journal of Computational Biology*, **2011**, 18(8), 997-1005.
[33] Krebs, B.B., De Mesquita, J.F. Amyotrophic lateral sclerosis type 20-in silico analysis and molecular dynamics simulation of hnrnpa1. *PloS One*, **2016**, 11(7), e0158939.
[34] Challa, B.R., Kantamneni, G.D., Suravajhala, M., Vadlamudi, S., Manne, M., Chathyushya, K. Phytochemical analysis and bioactive potential of moringa, eucalyptus, and nerium extracts against microbial, diabetic, inflammatory, and oxidative stress challenges. *3 Biotech*, **2025**, 15(11), 401.

HOW TO CITE THIS ARTICLE

H.A. Madkhali, M.N. Ansari, Y. Riadi, M.A. Ganaie, A.Y. Hamadi, N.M. Alhawiti. Evaluation of Apremilast as a Potential Inhibitor of Activated Factor XII: *In Vitro* and *In Silico* Approaches. *Adv. J. Chem. A*, 2026, 9(6), 1112-1127.

DOI: 10.48309/ajca.2026.566309.2009
URL: https://www.ajchem-a.com/article_238877.html